

## Electronic supplementary information (ESI)

### Tellurysulfide bond-launched redox-responsive superparamagnetic nanogel with acid-responsiveness for efficient anticancer therapy

Xiaoyang Xia, Xia Xiang,\* Fenghong Huang,\* Zhen Zhang, Ling Han

Oil Crops Research Institute of the Chinese Academy of Agricultural Sciences, Oil Crops and Lipids Process Technology National & Local Joint Engineering Laboratory, Key Laboratory of Oilseeds processing, Ministry of Agriculture, Hubei Key Laboratory of Lipid Chemistry and Nutrition, Wuhan 430062, China. *E-mail:* [xiangshi19850130@163.com](mailto:xiangshi19850130@163.com); [oiljgzx@gmail.com](mailto:oiljgzx@gmail.com).  
Tel: +86-27-86711526.

#### Materials and reagents

Sodium alginate (SA, Mw=32-250 kD), ethylenediamine dihydrochloride (EDC·HCl, 98 %), glycine (98.5%), Tellurium powder (Te, 99.8%), 11-bromoundecanoic acid (98%), and sodium borohydride (NaBH<sub>4</sub>, 98 %) were purchased from Aladdin Industrial Co. Iron (II) chloride tetrahydrate (FeCl<sub>2</sub>·4H<sub>2</sub>O, 98%), iron (III) chloride hexahydrate (FeCl<sub>3</sub>·6H<sub>2</sub>O, 97%) were purchased from Sigma-Aldrich. Dimethyl sulfoxide (DMSO) and tetrahydrofuran (THF) were purchased from Sinopharm Chemical Reagent. Doxorubicin hydrochloride (DOX·HCl, 98 %) was purchased from Arking Pharma Scientific. All the other chemicals and reagents used were analytical reagent grade.

#### Characterization

<sup>1</sup>H nuclear magnetic resonance (<sup>1</sup>H NMR) spectra were recorded on a Bruker Avance-500 spectrometer using D<sub>2</sub>O and d<sub>6</sub>-DMSO as solvent, respectively. The FT-IR spectra were recorded with a Nicolet 5700 spectrometer in the wavenumber range of 400-4000 cm<sup>-1</sup>. The size, size distribution, and zeta potential were investigated by dynamic light scattering (DLS) using a Zetasizer (Malvern Nano-ZS90) with a He-Ne laser beam at 633 nm at 25 °C. Morphology of nanocarrier was observed under a transmission electron microscope (TEM) using Tecnai G2S-Twin at an accelerating voltage of 200 kV. Around 5 μL of the nanocarrier suspension was placed on a copper grid. The grid was allowed to dry at room temperature overnight. The magnetic property of DOX-loaded nanocarrier was evaluated on a vibrating sample magnetometer (VSM, Westerville, OH, USA) via changing the magnetic field from -20000 to 20000 Oe at 25 °C. Intracellular fluorescence images of HeLa cells treated with MDTeSAN and free DOX were observed using confocal laser scanning microscopy (CLSM) (Nikon, TE2000, EZ-C1, Japan).

#### Synthesis of di-(1-carboxylundecyl) ditelluride (DTeDCA)

DTeDCA was synthesized according to the previous references with some modification.<sup>1, 2</sup> First, disodium ditelluride was prepared through reaction between telluride powder and sodium borohydride in water. Tellurium powder (3.75 g, 30 mmol) was added to 60 mL ice water containing dissolved sodium borohydride (5.04 g, 60 mmol) in a three-necked flask under a nitrogen atmosphere. The reaction mixture was stirred vigorously and reacted until the tellurium dissolved completely. Another quantity of tellurium powder (3.75 g, 30 mmol) was added. Then the mixture was heated to 50 °C for 30 minutes until a purple aqueous solution was obtained.

11-bromoundecanoic acid (15.84 g, 60 mmol) was dissolved in 40 mL of anhydrous THF. This was added to the purple aqueous solution above, with stirring overnight at 50 °C under nitrogen flow. After another 12 h of

stirring, the reaction mixture was filtered, and the obtained solution was extracted three times with 20 ml of CH<sub>2</sub>Cl<sub>2</sub> and dried with anhydrous MgSO<sub>4</sub>. The product was filtered, and then purified by re-crystallization from ethyl acetate. A brick red powder was obtained with a yield of 50.7 %.

#### **Synthesis of ditelluride bond modified alginate (SA<sub>STe</sub>COOH)**

SA<sub>STe</sub>COOH was synthesized by the exchange reaction between the sulfhydryl group of thiolated alginate (SA-SH) and the ditelluride group of DTeDCA according to the references with some modification.<sup>3, 4</sup> SA-SH was synthesized following previous work by amidation reaction between cysteamine and sodium alginate (SA).<sup>5, 6</sup> DTeDCA (0.050 g) in 10 mL DMSO was added to a three-necked flask under a nitrogen flow. SA-SH (0.125 g) dissolved in 10 mL phosphate solution (0.01 M, pH 6.56) was syringed dropwise into the above solution. The reaction mixture was stirred at 37 °C for 6 h. The resultant solution was dialyzed (MWCO 3500 Da) against DMSO for 48 h and then against ultrapure water for 48 h, finally lyophilized to obtain SA<sub>STe</sub>COOH as yellow powder. The chemical structure of SA<sub>STe</sub>COOH was confirmed by <sup>1</sup>HNMR and FT-IR.

#### **Preparation and characterization of magnetic DOX-loaded tellurysulfide bond modified alginate nanogel (MDTeSAN)**

Aminated SPION (SPION-NH<sub>2</sub>) was prepared following our previous work.<sup>7</sup> MDTeSAN was prepared through the electrostatic interaction between the carboxylic groups of SA<sub>STe</sub>COOH and the amino groups on DOX/SPION-NH<sub>2</sub>. In a typical procedure, SPION-NH<sub>2</sub> (4 mL, 1.25 mg/mL) with 0.25 mg of DOX was added dropwise to SA<sub>STe</sub>COOH solution (5 mL, 1 mg/mL). The suspension was stirred for 2 h at room temperature and then transferred into a dialysis bag (MWCO 3500 Da) to dialyze against ultrapure water to get rid of unencapsulated DOX and freeze-dried to obtain MDTeSAN, which was stored in 4 °C for further use. Magnetic DOX-free nanogel (MTeSAN) was prepared following the above procedure with the exception of DOX.

The sizes and zeta potentials of MDTeSAN were determined with DLS. The morphological examinations were carried out by TEM, and the magnetic property was evaluated on VSM. The amount of encapsulated DOX in the micelles was measured using a fluorescence spectrophotometer by recording the emission at 590 nm with excitation at 480 nm.<sup>5</sup> The drug loading content (DLC %) and drug encapsulation efficiency (DLE %) were calculated according to the following equations:

$$\text{DLC (\%)} = \frac{\text{weight of loaded DOX}}{\text{total weight of lyophilized nanogels}} \times 100 \%$$

$$\text{DLE (\%)} = \frac{\text{weight of loaded DOX}}{\text{weight of DOX in feed}} \times 100 \%$$

#### **GSH- and pH-triggered destabilization of MDTeSAN**

The GSH- and pH-sensitivity of MDTeSAN was assessed by dynamic light scattering (DLS). Briefly, freshly prepared MDTeSAN solutions were dispersed in PBS (0.01 M) at pH 7.4 or pH 5.0 without or with 10 mM GSH. The size changes of MDTeSAN were detected by DLS at different time points. Additionally, SA<sub>STe</sub>COOH and MDTeSAN solution were dispersed in PBS (0.01 M) at pH 7.4 with 10 mM GSH for 6 h and 10 h, and then were dialyzed against ultrapure water. The characterizations were confirmed by TEM, <sup>1</sup>HNMR and FT-IR.

#### **In vitro DOX release from MDTeSAN**

The in vitro release profiles of MDTeSAN were investigated in phosphate solution at different pH and GSH conditions using a dialysis-diffusion method. Briefly, 2 mL suspension of MDTeSAN was introduced into a dialysis bag (MWCO 3500 Da), which was immersed into 18 mL PBS (0.01 M) at pH 7.4 or pH 5.0 without or with 10 mM GSH. The release experiments were conducted in water bath with a shaking rate at 60 rpm at 37 °C. At predetermined intervals, 4.0 mL of the incubated solution was taken out and replaced with 4.0 mL of corresponding fresh buffer solution. The amount of DOX released was determined by fluorescence spectrometer. All measurements were performed in triplicate and presented as mean ± standard error (SE).

#### **Cytotoxicity assay**

The cytotoxicity of MTeSAN was measured in HeLa and NIH-3T3 cells by MTT assay, respectively. Cells were seeded into 96-well plates at a density of 5000 cells per well in 100 μL complete RPMI-1640 containing 10% FBS and cultured for 24 h at 37 °C in 5% CO<sub>2</sub> atmosphere. Then, cells were replaced with 200 μL complete RPMI 1640 medium containing plain nanogel at concentrations ranging from 1 to 75 μg mL<sup>-1</sup>. As a control, 200 μL fresh complete RPMI-1640 medium was applied. After 48 h incubation, the culture medium was disposed and cells were

washed thrice with PBS. Subsequently, 200  $\mu$ L culture medium including 20  $\mu$ L MTT solutions were added to each well with further incubation for 4 h. The medium was then replaced with 200  $\mu$ L DMSO to dissolve formazan crystal. Finally, the absorbance of samples was recorded using a microplate reader at 570 nm. The relative cell viability was calculated by comparing the absorbance in control wells with culture medium only. The data shown are the mean value of six replicates with a standard error ( $\pm$ SE).

HeLa cells were used to investigate the cytotoxicity of the magnetic DOX-loaded nanogels. HeLa cells were seeded into a 96 well plate at a density of 5000 cells per well and incubated in 5% CO<sub>2</sub> atmosphere at 37 °C for 24 h. The culture medium was then replaced with fresh medium containing free DOX and MDTeSAN with a DOX concentration ranging from 0.020 to 2.000  $\mu$ g/mL. Cells were allowed to incubate for 24 h and the cell viability were also determined by MTT assay. The experiments were conducted in six times and the results presented the average data.

External magnetic field was investigated as an additional factor on the cytotoxicity of various DOX-loaded nanogels (MDTeSAN M-: MDTeSAN under no magnetic field; MDTeSAN M+: MDTeSAN under magnetic field). A 0.3 T button permanent magnet with 10 mm in diameter and 3 mm in thickness was placed under the culture plate for magnetic targeting.<sup>8,9</sup> The relative cell viability (%) in reference to control wells was calculated according to the equation:

$$\text{Relative cell viability(\%)} = \frac{\text{Absorbance of sample} - \text{Absorbance of blank}}{\text{Absorbance of control} - \text{Absorbance of blank}} \times 100\%$$

Relative cell viability graphs were plotted against DOX concentrations for convenient comparison. Data were presented as average  $\pm$  SD (n=6).

#### **Cell uptake and intracellular distribution using confocal laser scanning microscopy (CLSM)**

CLSM was employed to visualize the intracellular distribution of DOX. In brief, HeLa cells were seeded in a glass-bottom dish with 1.5 mL of RPMI-1640 growth medium. After 24 h of incubation at 37 °C, the attached cells were then incubated with free DOX, MDTeSAN M-, and MDTeSAN M+ for another 4 h or 12 h at 37 °C. At predetermined time, the cells were washed with PBS, incubated with Hoechst 33258 solution at 37 °C for 10 min for nuclei staining and then rinsed with PBS. Finally, all the cell samples were observed by the CLSM (Nikon, TE2000, EZ-C1, Japan).

#### ***In Vivo* antitumor efficacy**

The inhibitory activities in tumor growth were assessed with BABL/c mice (female 5-6 weeks old, animal experiment center of Wuhan University, China) following our previous methods.<sup>6</sup> H22 cells ( $\sim 5 \times 10^6$  cells/each mouse) were subcutaneously transplanted into the female mice. When the tumors grew to an average size of about 80 mm<sup>3</sup>, the mice were randomly divided into four groups (n=4), and intravenously administered via tail vein with PBS, free DOX and MDTeSAN at a dose of 3.33 mg (DOX) per kg (body weight) weekly, respectively. The body weight of the mice and tumors were measured every two day. At 30th day, the mice were sacrificed by cervical decapitation. A 0.3 T button permanent magnet with 10 mm in diameter and 3 mm in thickness was placed under the tumor sites of mice. The developed tumor was monitored with a caliper in two dimensions and the tumor volume (V) calculated as follows:

$$V = \frac{\text{the longest diameter of tumor} \times (\text{the shortest diameter of tumor})^2}{2}$$

The tumor size was expressed as an arithmetic means with a standard error.

The tumor growth inhibition rate (IR) was calculated as follows:

$$\text{IR(\%)} = 1 - \frac{\text{weight of tumor in the experimental group}}{\text{weight of tumor in the control group}} \times 100\%$$

#### **Histological Staining**

At day 30, the tumors and major organs (heart, liver, spleen, lungs and kidneys) were removed and fixed in 4% PBS buffered paraformaldehyde for 24 h and then embedded in paraffin. The paraffin embedded tissues were sliced at 5  $\mu$ m thickness and then stained with hematoxylin-eosin (H&E) and with prussian blue for histological alterations assessment by the microscopy (Olympus IX51/Q-IMAGING Micro Publisher).

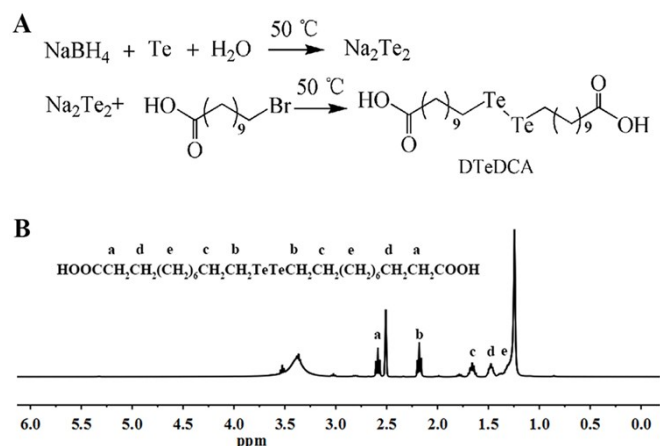


**Fig. S1** (A) Synthesis route of DTeDCA, (B)  $^1\text{H}$ NMR spectrum of DTeDCA using  $\text{d}_6\text{-DMSO}$  as a solvent.

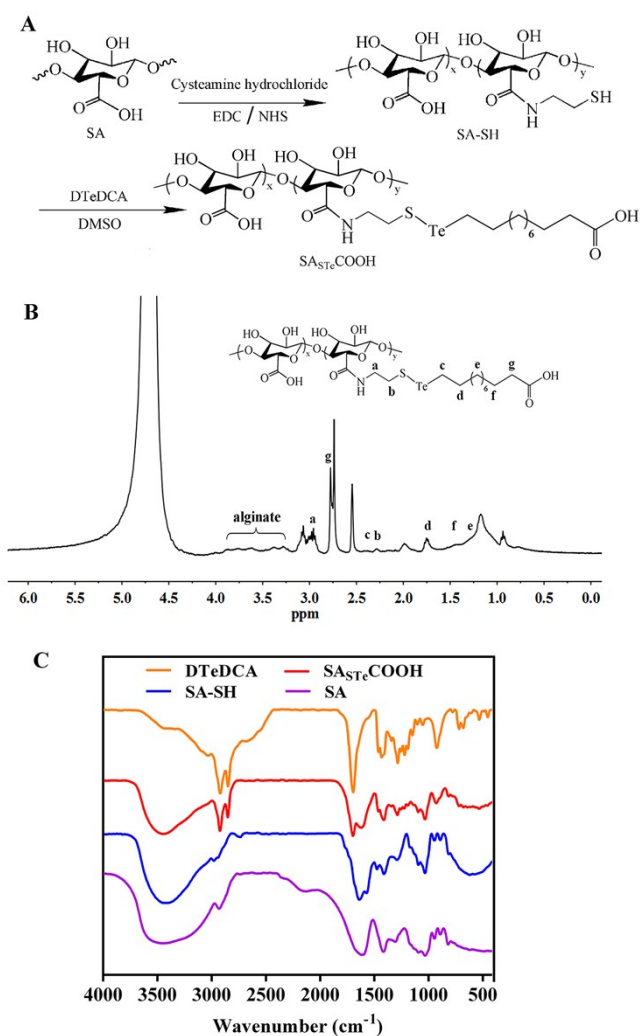


**Fig. S2** (A) Synthesis route of  $\text{SA}_{\text{STeCOOH}}$ , (B)  $^1\text{H}$ NMR spectrum of  $\text{SA}_{\text{STeCOOH}}$  using  $\text{D}_2\text{O}/\text{d}_6\text{-DMSO}$  (V/V: 10/1) as a solvent, (C) FT-IR spectra of DTeDCA, SA, SA-SH, and  $\text{SA}_{\text{STeCOOH}}$ .

First,  $\text{SPION-NH}_2$  was prepared via the formation of Fe-O-C bond<sup>6</sup>. The average hydrodynamic size of  $\text{SPION-NH}_2$  was determined to be  $21.6 \pm 1.7$  nm by DLS method, with zeta potential of  $+28.3 \pm 0.4$  mV. These data were in agreement with the previous result.<sup>6</sup> The synthesis route and  $^1\text{H}$ NMR measurement of DTeDCA were shown in Fig. S1A and Fig. S1B. The  $^1\text{H}$ NMR showed that the peaks at 2.68 ppm (t, 4H), 2.45 ppm (t, 4H), 1.72 ppm (m,

4H), 1.45 ppm (m, 4H), and 1.43-1.26 ppm (m, 24H) corresponded to  $\text{CH}_2\text{COOH}$ ,  $\text{TeCH}_2$ ,  $\text{TeCH}_2\text{CH}_2$ ,  $\text{CH}_2\text{CH}_2\text{COOH}$ , and  $(\text{CH}_2)_6\text{CH}_2\text{CH}_2\text{COOH}$ , respectively. The results were in agreement with the reference,<sup>10</sup> indicating the successful synthesis of DTedCA. SA-SH was synthesized and characterized following our previous references.<sup>6</sup> On the other hand, the amount of thiol groups introduced in the thiolation process was measured by the Ellman's Test. The quantitative determination results demonstrated that the degree of -SH group was calculated to be 20% based on the content of carboxylic groups. The synthetic route of  $\text{SA}_{\text{STe}}\text{COOH}$  was shown in Fig. S2A. The chemical structure was characterized by  $^1\text{H}$ NMR spectrum (Fig. S2B) and FT-IR spectrum (Fig. S2C). The chemical shifts at between 3.60 and 3.96 ppm belonged to the typical frame vibration of SA. The peak a (2.90 ppm) and peak b (2.35 ppm) corresponded to the methylene protons of  $-\text{CONHCH}_2\text{CH}_2-$  group. In addition, the peak g (3.05 ppm), peak c (2.45 ppm) and peak d (1.71 ppm), peak f (2.38 ppm) peak e (1.42-1.25 ppm) were assigned to the methylene protons, which were consistent with characteristic signals of DTedCA. In the FT-IR spectra (Fig. 1C), the bands at  $1710\text{ cm}^{-1}$ ,  $2920$  and  $2850\text{ cm}^{-1}$ ,  $1020\text{ cm}^{-1}$  indicated the  $\text{C}=\text{O}$ ,  $-\text{CH}_2-$ , and  $\text{C}-\text{O}-\text{C}$  stretching,<sup>11, 12</sup> respectively. These results further verified the successful synthesis of DTedCA. The appearance of two peaks  $1725$  and  $1560\text{ cm}^{-1}$  belonged to the  $-\text{CONH}-$  stretching bonds in SA-SH.<sup>6</sup> The  $\text{SA}_{\text{STe}}\text{COOH}$  combined characteristic signals and bonds of both DTedCA and SA-SH, indicating the successful preparation.

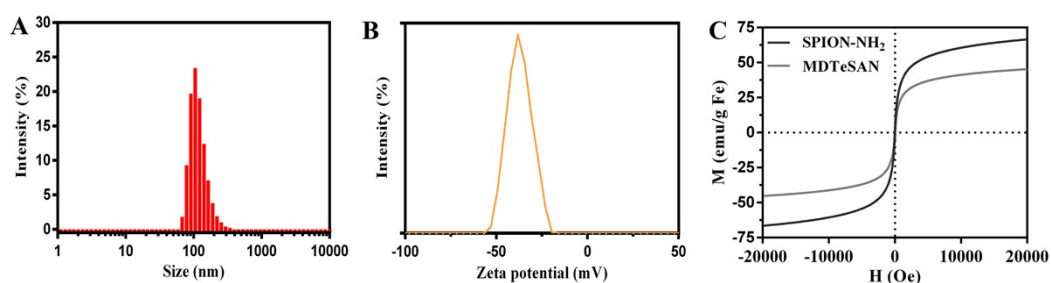


**Fig. S3** The size distribution by DLS of MDTeSAN (A), zeta potential of MDTeSAN (B), and vibrating sample magnetometer (VSM) of SPION-NH<sub>2</sub> and MDTeSAN at ambient temperature (C).

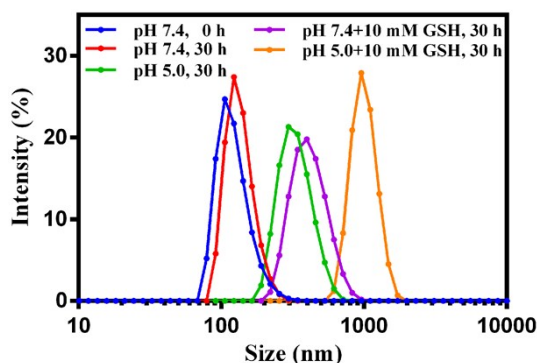


**Fig. S4** Size change of plain nanogels exposed to different environments: 0.01 M PBS of pH 7.4 and pH 5.0 with or without 10 mM GSH at different time.

Fig. S4 displayed the size changes of plain nanogels in different medium. In pH 7.4 PBS buffer, both the size and size distribution of nanogels varied slightly during the period of 30 h, even displaying slight variation over one month (data not shown). It turned out that nanogels catered for the primary requirements in biomedical applications. Due to the conjugation between copious carboxylic groups and DOX or SPION-NH<sub>2</sub>, the formed nanogels were in negatively charged, allowing long storage stability. When nanogels were exposed to pH 5.0, the size increased and precipitation was observed after 30 h. The reason might be ascribed to that mildly acidic medium neutralized the carboxylic group-originated negative surface charge of nanogels and thus electrostatic interaction was attenuated. When 10 mM GSH was applied in pH 5.0 PBS, a notable increase in size and obvious precipitation was observed after 30 h. As well, GSH induced the cleavage of tellurysulfide bond. The feature of disassembly in both acidic and reductive environments predicted the GSH- and pH-triggered release.

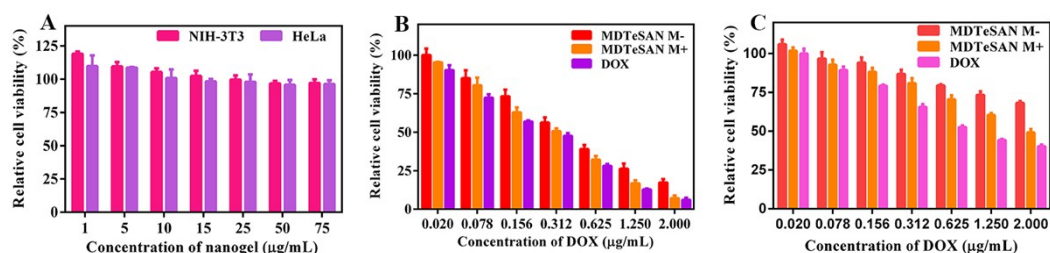


**Fig. S5** (A) Biocompatibility of plain nanogels against HeLa and NIH-3T3 cells after 48 h incubation. Cytotoxicity comparison of (B) free DOX and MDTeSAN between against HeLa cells after 48 h incubation, (C) free DOX, MDTeSAN M-, and MDTeSAN M+ against NIH-3T3 cells after 48 h.

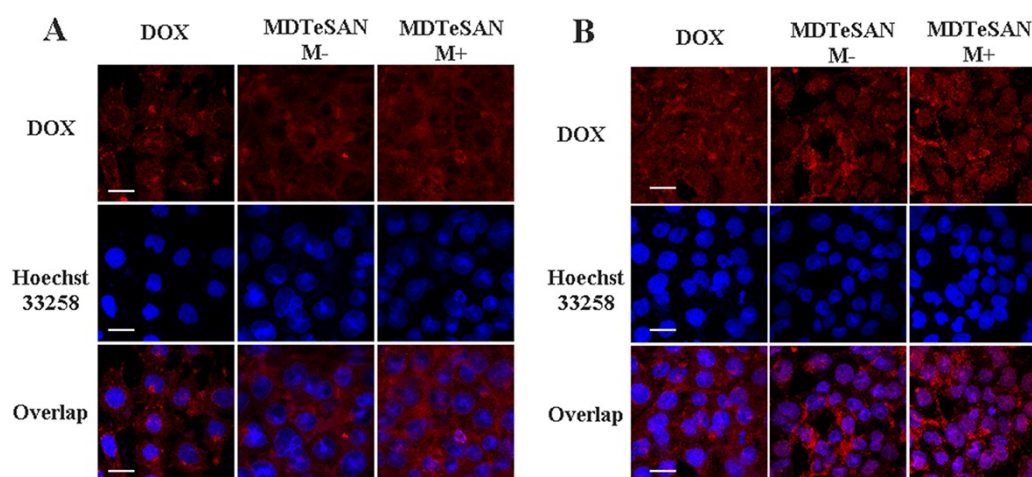


**Fig. S6** CLSM images of HeLa cells treated with MDTeSAN M-, MDTeSAN M+ and free DOX by HeLa cells at a DOX concentration of  $0.20 \mu\text{g mL}^{-1}$  using confocal laser scanning microscopy (CLSM) for respective 4 h (A) and 12 h (B) incubation (Scale bars:  $20 \mu\text{m}$ ). Blue was cell nucleus treated with Hoechst 33258. Red is the fluorescence of DOX. The last column was their overlap.

To further demonstrate whether MDTeSAN can be more efficiently internalized, experiments on the intracellular study of MDTeSAN were performed on HeLa cells after treatment for 4 or 12 h by CLSM analysis. As shown in Fig. S6A, red DOX fluorescence was observed in the cells after 4 h incubation. After 12 h incubation with free DOX (Fig. S6B), more DOX fluorescence was located in both cytoplasm and nuclei. In contrast, cells incubated with MDTeSAN for 12 h, the fluorescence intensities of DOX were increased compared to that of 4 h, demonstrating the restrictive DOX release function of nanogels. Besides, DOX was visualized and accumulated obviously in nuclei after 12 h incubation, indicating the enhanced endocytosis of nanogels to transfer released DOX inside the cytoplasm into the nuclei. It was suggested that the electrovalent bonds between the negative carboxyl groups and the positive amine groups were dissociated by the mild acid environment in cytoplasm as well as the tellurysulfide linkage was cleaved by intracellular GSH concentration. Meanwhile, with 12 h incubation, the accumulation of DOX released from MDTeSAN M+ became more evident compared to that from MDTeSAN M-, displaying stronger binding ability of MDTeSAN M+ with HeLa cells than MDTeSAN M-. It indirectly demonstrated that MDTeSAN under the external magnetic field was quickly internalized to HeLa cells and released more DOX to nuclei, finally achieving enhanced inhibition effects.

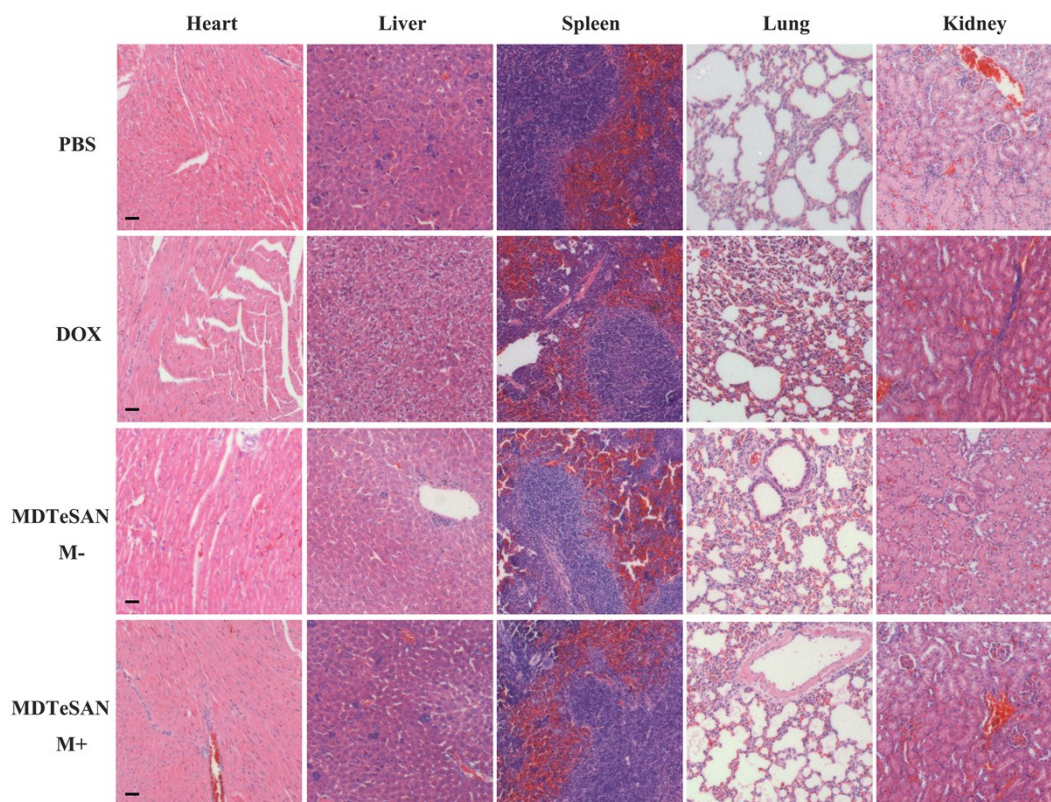


**Fig. S7** H&E stained tissue sections from the heart, liver, spleen, lung, and kidney after 30 days post-treatment of chemophotodynamic combination therapy. (Scale bars: 20  $\mu$ m).

The H & E staining assessments of tissue sections of vital organs were explored to evaluate the toxicology of the nanogels. As shown in Fig. S7, H&E staining of the heart tissues in free DOX group exhibited obvious signals of myocardial inflammation, and similar variation trends were observed in the liver tissues, which revealed significant hepatotoxicity with cytoplasmic relaxation, nucleus degeneration and apoptosis. These phenomena were resulted from toxic and side effect of free DOX.<sup>13</sup> However, H&E staining analysis of heart, liver, spleen, lung, and kidney tissues revealed that no apparent damage or toxicity was observed in the PBS, MDTeSAN M-, and MDTeSAN M+ treated groups, revealing that MDTeSAN would produce low systemic adverse effect. All *in vivo* results demonstrated that the MDTeSAN as a redox- and acid-responsive superparamagnetic nanogel had toxicity as low as PBS.

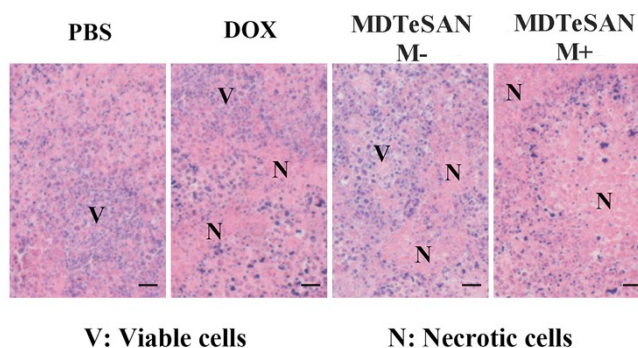


**Fig. S8** Representative images of tumor sections for the confirmation of antitumor activity by H & E staining (Scale bars: 20  $\mu$ m).

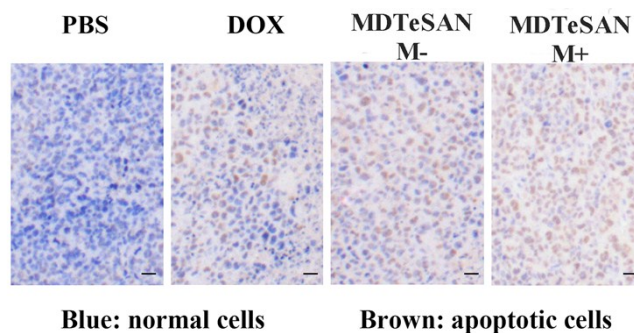


**Fig. S9** Representative images of tumor sections by TUNEL staining (Scale bars: 20  $\mu\text{m}$ ).

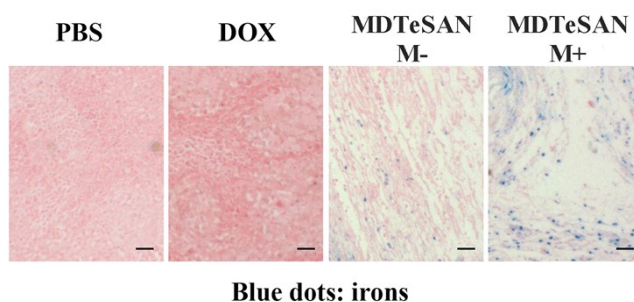


**Fig. S10** Representative images of tumor sections by Prussian blue staining (Scale bars: 20  $\mu\text{m}$ ).

To confirm the antitumor efficacy induced by this targeted therapy, Fig. S8 showed the H&E staining of the tumor samples following treatment with control (PBS), DOX and MDTeSAN, respectively. Compared to PBS treated group, necrotic regions were typically observed within the tumor samples of mice treated with DOX and MDTeSAN, demonstrating inhibitory effect against the growth of H22 liver tumor cells *in situ*. Notably, MDTeSAN M+ induced more remarkable necrosis in the tumors than MDTeSAN M-, exhibiting that external magnetic field could enhance the drug release efficiency of MDTeSAN at the tumor site. TUNEL assay also obtained the same conclusions. Fig. S9 showed cell apoptosis at different extent treated with DOX and MDTeSAN, especially MDTeSAN M+, displaying massive dark brown cells with nuclei lysis and cell breakage.<sup>8, 14-15</sup> In addition, the *in vivo* accumulation and distribution of MDTeSAN were confirmed by tracking the iron, as shown in Fig. S10. Prussian blue staining analysis showed that no iron (blue dots) in the tumor tissue was observed when the tumor samples were treated with PBS and free DOX, while obvious accumulation and distribution were found in the tumor tissue treated with MDTeSAN M- and MDTeSAN M+, especially MDTeSAN M+. These results indicated that MDTeSAN had higher antitumor therapeutic efficacy than free DOX.

**Table S1.** The half maximal inhibitory concentration ( $IC_{50}$ ) of free DOX, MDTeSAN M- and MDTeSAN M+ against NIH-3T3 and HeLa cells for 48 h incubation.

| Samples       | $IC_{50}$ ( $\mu\text{g mL}^{-1}$ ) |                 |                 |
|---------------|-------------------------------------|-----------------|-----------------|
|               | Free DOX                            | MDTeSAN M-      | MDTeSAN M+      |
| NIH-3T3 cells | $0.77 \pm 0.08$                     | -               | $1.86 \pm 0.22$ |
| HeLa cells    | $0.28 \pm 0.03$                     | $0.40 \pm 0.05$ | $0.32 \pm 0.07$ |

## Notes and references

1. N. Ma, Y. Li, H. Xu, Z. Wang and X. Zhang, *J. Am. Chem. Soci.*, 2010, **132**, 442-443.
2. Y. Wang, L. Zhu, Y. Wang, L. Li, Y. Lu, L. Shen and L. Zhang, *ACS Appl. Mater. Interfaces*, 2016, **8**, 35106-35113.
3. P. O. Amoako, P. C. Uden and J. F. Tyson, *Anal. Chim. Acta*, 2009, **652**, 315-323.
4. D. Steinmann, T. Nauser and W. H. Koppenol, *J. Org. Chem.*, 2010, **75**, 6696-6699.
5. J. Huang, Y. Xue, N. Cai, H. Zhang, K. Wen, X. Luo, S. Long and F. Yu, *Mat. Sci. Eng. C*, 2015, **46**, 41-51.
6. L. Chen, Y. Xue, X. Xia, M. Song, J. Huang, H. Zhang, B. Yu, S. Long, Y. Liu and L. Liu, *J. Mater. Chem. B*, 2015, **3**, 8949-8962.
7. H. Zhang, Y. Xue, J. Huang, X. Xia, M. Song, K. Wen, X. Zhang, X. Luo, N. Cai and S. Long, *J. Mater. Sci.*, 2015, **50**, 2429-2442.
8. Z. Tang, L. Zhang, Y. Wang, D. Li, Z. Zhong and S. Zhou, *Acta Biomater.*, 2016, **42**, 232-246.
9. B. Ramaswamy, S. D. Kulkarni, P. S. Villar, R. S. Smith, C. Eberly, R. C. Araneda, D. A. Depireux and B. Shapiro, *Nanomed. Nanotechnol.*, 2015, **11**, 1821-1829.
10. D. Wakamatsu, S. Morimura, T. Sawa, K. Kida, C. Nakai and H. Maeda, *Biosci. Biotech. Bioch.*, 2005, **69**, 1568-1574.
11. D. Wang, J. Zhou, R. Chen, R. Shi, C. Wang, J. Lu, G. Zhao, G. Xia, S. Zhou and Z. Liu, *Chem. Mater.*, 2017, **29**, 3477-3489.
12. J. P. de Mesquita, C. L. Donnici and F. V. Pereira, *Biomacromolecules*, 2010, **11**, 473-480.
13. Y. Zhang, H. Fan, C. Ren, L. Yang, J. Liu, C. Zhen, L. Chu and J. Liu, *ACS Appl. Mater. Interfaces*, 2017, **9**, 13016-13028.
14. J. Li, Y. Hu, J. Yang, P. Wei, W. Sun, M. Shen, G. Zhang and X. Shi, *Biomaterials*, 2015, **38**, 10-21.
15. W. Wang, D. Cheng, F. Gong, X. Miao and X. Shuai, *Adv. Mater.*, 2012, **24**, 115-120.